Effects of Salt on Polyelectrolyte−Micelle Coacervation

Yilin Wang, Kozue Kimura, Qingrong Huang, and Paul L. Dubin*

Department of Chemistry, Indiana University-Purdue University, Indianapolis, Indiana 46202

Werner Jaeger

Fraunhofer-Institut fuer Angewandte Polymerforschung, D-14513 Teltow, Germany

Received June 18, 1999; Revised Manuscript Received August 16, 1999

ABSTRACT: Turbidity, dynamic light scattering, and electrophoretic mobility were used to study the effects of added salt on coacervation in the system composed of the strong cationic polymer poly(diallyldimethylammonium chloride) (PDADMAC) and oppositely charged mixed micelles of Triton X-100 (TX100) and sodium dodecyl sulfate (SDS). The phase behavior in the range of ionic strengths from 0.05 to 0.60 M includes regimes of soluble complex formation, coacervation, and precipitation. The corresponding phase boundaries are determined from differential turbidity curves. The shift of the phase boundaries to higher ratios of SDS:TX100 with increase in salt concentration is explained on the basis of electrostatic screening. The width of the coacervation region is found to increase with ionic strength. These observations are consistent with previous reports of the "salt suppression" and "salt enhancement" of coacervation. In the coacervation region, the electrophoretic mobility is found to be close to zero. At higher and lower ionic strengths, soluble complexes are positively or negatively charged, respectively. It is suggested that the principal factor governing coacervation in this system is electroneutrality of the polyion−micelle complex which in turn depends on the charge and number of bound micelles.

Introduction

Coacervation is a phenomenon in which a macromolecular aqueous solution separates into two immiscible liquid phases. The more dense phase, which is relatively concentrated in macromolecules, is called the coacervate and is in equilibrium with the relatively dilute macromolecular liquid phase.[1] This liquid−liquid phase separation has been widely used in cosmetic formulations[2] and pharmaceutical microencapsulations.[3,4] Owing to these widespread technical applications and to some fascinating biological implications,[5] coacervation is an intriguing but underexamined topic of investigation.[6,7]

The phenomenon can be divided into "simple" and "complex" coacervation. The former involves only one macromolecule and may result from the addition of a dehydrating agent that promotes polymer−polymer interactions over polymer−solvent interactions. In the latter, two or more oppositely charged macromolecules or colloidal species are present. For this case, Piculell and Lindman[8] have recommended the term "associative phase separation" to replace "complex coacervation".

Complex coacervation may be exhibited by polyelectrolytes and colloids. One example is polyelectrolytes interacting strongly with oppositely charged micelles, normally leading to phase separation.[8−13] Such mixtures may form a single phase either without complex formation or with soluble complex, liquid−liquid-phase separation (coacervation), or liquid−solid phase separation (precipitation). In particular, we have studied the system composed of the strong polycation poly(diallyldimethylammonium chloride) (PDADMAC) and oppositely charged mixed micelles of Triton X-100 (TX100) and sodium dodecyl sulfate (SDS) by many experimental methods, including turbidimetry,[14,15] dynamic and static light scattering,[16−18] viscometry,[18] electrophoretic light scattering,[18] microcalorimetry,[19] dye solubilization,[20] and equilibrium dialysis.[18] These studies revealed the existence of several phase states, including coacervate and soluble complexes, depending inter alia on the mixing ratio of PDADMAC and TX100-SDS.

In polyelectrolyte−micelle systems, or in binary polyelectrolyte mixtures, coacervation is primarily controlled by electrostatic forces. The complex factors influencing coacervation may include polymer molecular weight, concentration, and molecular geometry; micelle size and concentration; and polymer:micelle stoichiometry.[8,9] However, electrostatic factors, such as macromolecular charge densities and ionic strength, are most significant. Whether or not complex coacervation takes place appears to depend mainly on the micelle surface charge density, the polymer linear charge density, and the Debye−Hückel ion-atmosphere thickness.[15,21,22] At very low charge densities, coacervation is suppressed,[23] and at very high charge densities, precipitation may occur.[24] In the case of polyelectrolytes and micelles of opposite charge, the charge densities of the latter are controlled by the mixing ratio of nonionic and ionic surfactants.[14−18,25−32]

The addition of salt has a significant effect on coacervation of polyelectrolytes and oppositely charged micelles[8] due to screening of the interaction between these two components. Some investigators[33−37] have reported that the interaction between polyelectrolytes and oppositely charged micelles is reduced by addition of salt, which is indicated by an increase in the critical aggregation concentration (cac) with increased salt concentration. Since the phase behavior of such systems is a reflection of these interactions, it must be influenced by added salt. The salt effect on the phase behavior of a system containing a micellar cationic surfactant, tetradecyltrimethylammonium bromide, and an anionic polyelectrolyte, polysaccharide sodium hyaluronate, was investigated by Thalberg et al.[38] They observed a strong diminution of the two-phase region, i.e., a decrease in the coacervation region in the presence of salt relative to the salt-free system. Guillemet and Piculell[11] inves-

10.1021/ma990972v CCC: $18.00
Published on Web 09/29/1999

tigated aqueous mixtures of micellar SDS with a cellulose derivative substituted with hydrophobic side chains in the absence and in the presence of salt. In apparent contrast to the results obtained by Thalberg et al., Guillemet and Piculell indicated that coacervation occurs earlier in the presence of salt; i.e., coacervation is shifted to lower surfactant concentration. These findings suggest that coacervation can be both suppressed and enhanced by added salt, an effect not well understood. This illustrates the point that much work remains to be done to further understand the coacervation of polyelectrolyte/surfactant systems and consequently to exploit them.

The PDADMAC/TX100-SDS system mentioned above may provide a model system by means of which the effect of salt on coacervation can be addressed. Our previous studies[14−18,25−32] have indicated that the strong electrostatic interaction between polyion and micelle could be attenuated by using mixed micelles of nonionic and ionic surfactants, with the charge density of the mixed TX100-SDS micelles adjusted via the molar ratio of ionic to nonionic surfactant. This suggested to us that coacervates of PDADMAC/TX100-SDS should be formed over a wide range of conditions, facilitating a systematic study of the effect of salt on coacervation. Therefore, in the present paper, the effect of salt on coacervation in the PDADMAC/TX100-SDS system is investigated by turbidimetric titration, dynamic light scattering, and mobility measurement. The purpose of these studies is to understand the reported salt suppression and salt enhancement of coacervation and to gain further insight into the mechanism of coacervation.

Experimental Section

Materials. Poly(diallydimethylammonium chloride) (PDADMAC) was prepared by free radical aqueous polymerization of diallydimethylammonium chloride.[39] The average molecular weight (M_n) of the purified lyophilized polymer was determined by membrane osmometry as 2.7×10^5. Triton X-100 (TX100) was purchased from Aldrich, sodium dodecyl sulfate (SDS, purity>99%) from Fluka, and NaCl from Fisher. All were used without further purification. Distilled water was used in all experiments.

Turbidimetric Titrations. Turbidity measurements, reported as $100 - \%T$, were performed at 420 nm using a Brinkman PC800 probe colorimeter equipped with a 2 cm path length fiber optics probe. Turbidimetric "type 1" titrations were carried out at 26 ± 1 °C by adding 60 mM SDS in 0.05, 0.10, 0.20, 0.40, and 0.60 M NaCl to solutions of TX100 and PDADMAC with initial concentration of 20 mM and 1 g/L also at the same NaCl concentrations, to bring the solutions to different Y values. Y is defined as

$$Y = \frac{[\mathrm{SDS}]}{[\mathrm{SDS}] + [\mathrm{TX100}]} \tag{1}$$

which is proportional to the average mixed micelle surface charge density. To fix the concentrations of TX100 and PDADMAC to be 20 mM and 1 g/L, turbidimetric titration was carried out by adding equal volumes of 60 mM SDS and a solution of 40 mM TX100 and 2 g/L PDADMAC in 0.1 M NaCl to a solution of 20 mM TX100 and 1 g/L PDADMAC also in 0.1 M NaCl. All measured values were corrected by subtracting the turbidity of a polymer-free blank.

Dynamic Light Scattering. All measurements were carried out at a scattering angle of 90° and at 26.0 ± 0.5 °C with a DynaPro-801 (Protein Solutions Inc., Charlottesville, VA), which employs a 30 mW solid-state 780 nm laser and an avalanche photodiode detector. Samples with 1 g/L PDADMAC and 20 mM TX100 in 0.10 M NaCl at desired Y values were prepared and were stirred for at least 2 h before measurements. The samples were introduced into the 7 μL cell through a 0.20 μm filter prior to measurement. The correlation function of the scattering data was analyzed via the method of regularization[40] and then used to determine the diffusion coefficient D of the solutes. The diffusion coefficient D can be converted into the hydrodynamic radius R_h using the Stokes−Einstein equation

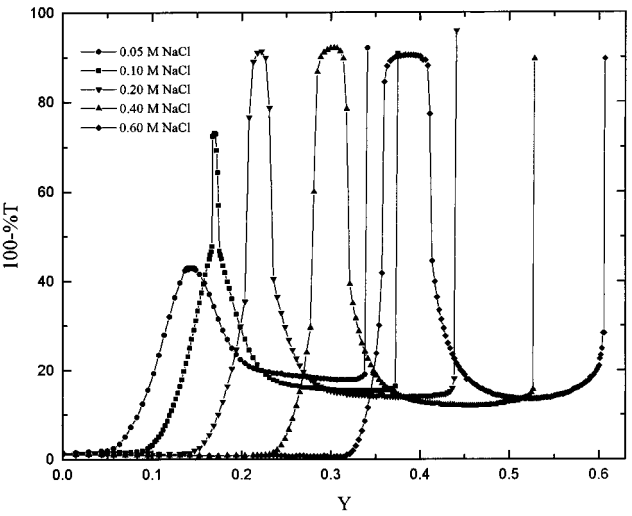

Figure 1. Turbidity of PDADMAC/TX100−SDS as a function of Y in 0.05, 0.10, 0.20, 0.40, and 0.60 M NaCl.

$$R_h = \frac{kT}{6\pi\eta D} \tag{2}$$

where k is the Boltzmann constant, T is the absolute temperature, and η is the solvent viscosity.

Mobility Measurement. Electrophoretic mobility was measured using a ZetaPALS (Brookhaven Instruments), the operation of which is based on the principles of phase analysis light scattering.[41] The 1 cm square sample cell, thermostated by a Peltier device, contains electrodes which provide a field that can be reversed automatically and is remote from any cell wall. The cell can be driven by fields of up to 60 kV m^{-1} at either square or sine wave frequencies from dc to >1 MHz. A laser beam is split to produce a scattering beam and a reference beam, which can be modulated by a piezoelectric phase modulator at frequencies from 62.5 to 2000 Hz. The ratio of scattered to reference signal is optimized by automatic adjustment of a continuous attenuator in the incident beam path. Further details about the technique can be found in ref 42. The samples with 1 g/L PDADMAC and 20 mM TX100 in 0.10 M NaCl at desired Y values were stirred for at least 2 h before measurements and measured at 26.0 ± 0.2 °C.

Results and Discussion

"Type 1" turbidimetric titration curves of PDADMAC+TX100 with SDS at 0.05, 0.10, 0.20, 0.40, and 0.60 M NaCl are shown in Figure 1. The initial concentrations of PDADMAC and TX100 are 1 g/L and 20 mM, respectively. The turbidity is constant and very small at low Y values. The well-defined point of initial turbidity increase is designated as Y_c, beyond which the turbidity increases gradually with increase of Y. For I > 0.05 M, Y_c is followed by an abrupt increase in turbidity and extremely large turbidities at $Y_{\phi 1}$, following which coacervation is demonstrated by centrifugation (30 min at 25 °C and 3000 rpm) yielding two liquid phases. Maxima with respect to Y are subsequently observed which shift from left to right (to larger Y) with increase of salt concentration. Further addition of SDS causes the coacervate to redissolve at $Y_{\phi 2}$ accompanied by a decrease in turbidity. Beyond $Y_{\phi 2}$, coacervate does

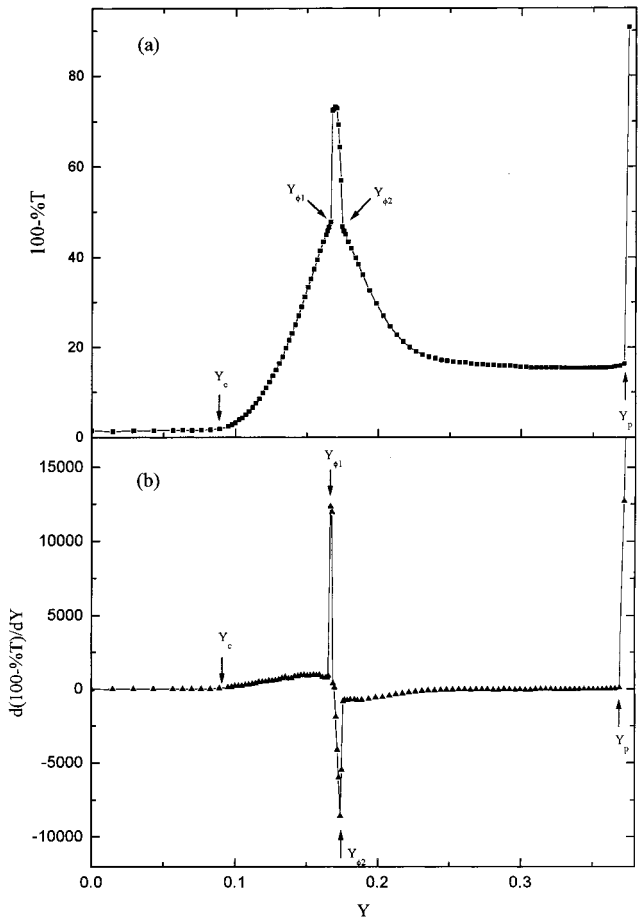

Figure 2. (a) Turbidity and (b) differential turbidity of PDADMAC/TX100−SDS as a function of Y in 0.10 M NaCl.

not exist. Thus, the interval between $Y_{\phi 1}$ and $Y_{\phi 2}$ is the coacervation region. At $Y > Y_{\phi 2}$, the turbidity continues to decrease and then becomes constant. Finally, a sharp increase in turbidity at Y_p signals precipitation. For the conditions of Figure 1, i.e., polymer residue concentration of 6.2 mM, an equivalent concentration of anionic surfactant would obtain at $Y = 0.24$. It does not appear that such simple bulk stoichiometry has any particular significance for the phase behavior.

These phase boundaries can be operationally identified more precisely by differentiating the above turbidity curves as demonstrated for $I = 0.10$ M in Figure 2. The sharp changes in d(100% − T)/dY shown in Figure 2b correspond to phase changes. The results at various ionic strengths are summarized in the two-dimensional "phase diagram" of Figure 3, expressing the dependences of Y_c, $Y_{\phi 1}$, $Y_{\phi 2}$, and Y_p on salt concentration. Since Figure 3 only tells us at what condition coacervation takes place, but not the composition of the two phases at coacervation, they are strictly speaking phase boundaries, not phase diagrams. Ternary phase diagrams have been mainly employed by Piculell and Lindman[8,13] to describe phase behavior of polymer−surfactant systems with reference to binary phase equilibrium. However, in our case, the components, including polyelectrolyte, nonionic surfactant, ionic surfactant, salt, and water, are all variable during phase separation, which greatly complicates the determination of compositions in such multidimensional phase diagrams. Nevertheless, the present simplified phase boundaries are still quite informative. In domain I, a single phase exists in the absence of interaction between polymer and micelles. In region II, the binding of TX100−SDS micelles with PDADMAC leads to soluble complexes without phase separation. Liquid−liquid phase separation, i.e. coacervation, takes place in region III. In region IV, the addition of excess anionic surfactant leads to coacervate redissolution and re-formation of a single soluble complex phase. Region V corresponds to liquid−solid phase separation, i.e. precipitation. All of phase boundaries (Y_c, $Y_{\phi 1}$, $Y_{\phi 2}$, and Y_p) are shifted to larger Y values with added salt. The coacervation region widens with the increase of salt concentration. The proximity of the II/III and III/IV boundaries at low I suggests the presence of a critical point in the vicinity of $0.05 < I < 0.10$.

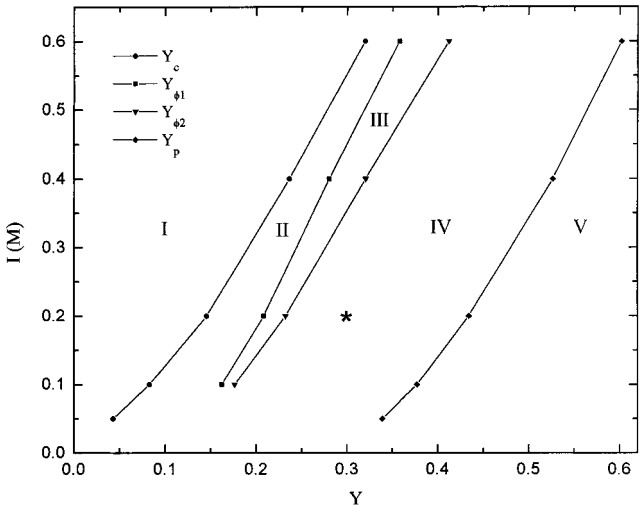

Figure 3. Phase boundaries of the PDADMAC/TX100−SDS system at 0.05, 0.10, 0.20, 0.40, and 0.60 M NaCl.

The phase diagram in Figure 3 suggests that the phase behavior could be changed by either increase or decrease in salt concentrations. For examples, when $0.16 < Y < 0.42$ and the system is located in coacervation region III, decrease or increase of salt concentration could move the system into region IV or region II, respectively; when $0.16 < Y < 0.36$ and the system is located in region I or II, decrease of salt concentration could move the system into coacervation region III; when $0.16 < Y < 0.42$ and the system is located in region IV, increase of salt concentration could also move the system into the coacervation region III. In other words, coacervation could be enhanced and suppressed by changing salt concentration. To provide direct evidence for this behavior, "titration" with concentrated NaCl solution was carried out for the system of 1 g/L PDADMAC and 20 mM TX100-SDS at $Y = 0.3$. The initial point at salt concentration 0.2 M is located in region IV, indicated in Figure 3 by "*". As shown in Figure 4, the turbidity increases with the addition of salt, and a sharp increase is observed when the system goes into coacervation region III at $I = 0.34$ M. When the salt concentration reaches 0.42 M, the turbidity decreases abruptly as coacervates are redissolved, and the system goes into region II. This result indicates that coacervation can indeed be both enhanced and suppressed by changing salt concentration.

Insight into the structure of the complexes and coacervates may be obtained from the results of dynamic light scattering and mobility measurements. Figure 5a−c shows complex size, mobility, and turbidity as a function of Y in 0.10 M NaCl, at 1 g/L polymer and 20 mM total surfactant. At $Y < Y_c$ (region I), the size is

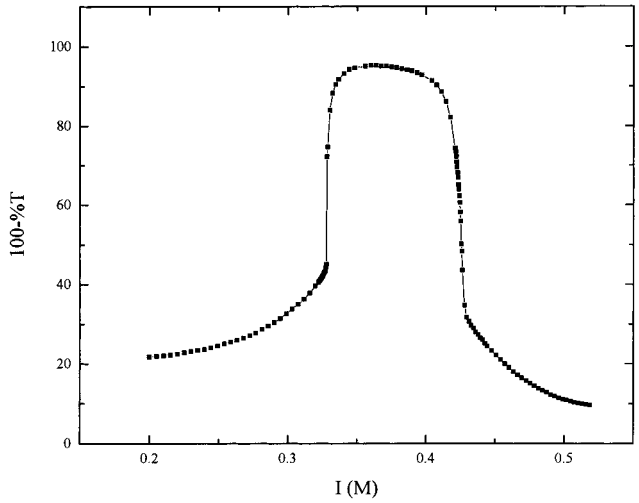

Figure 4. Turbidity of PDADMAC/TX100−SDS as a function of salt concentration at $Y = 0.30$.

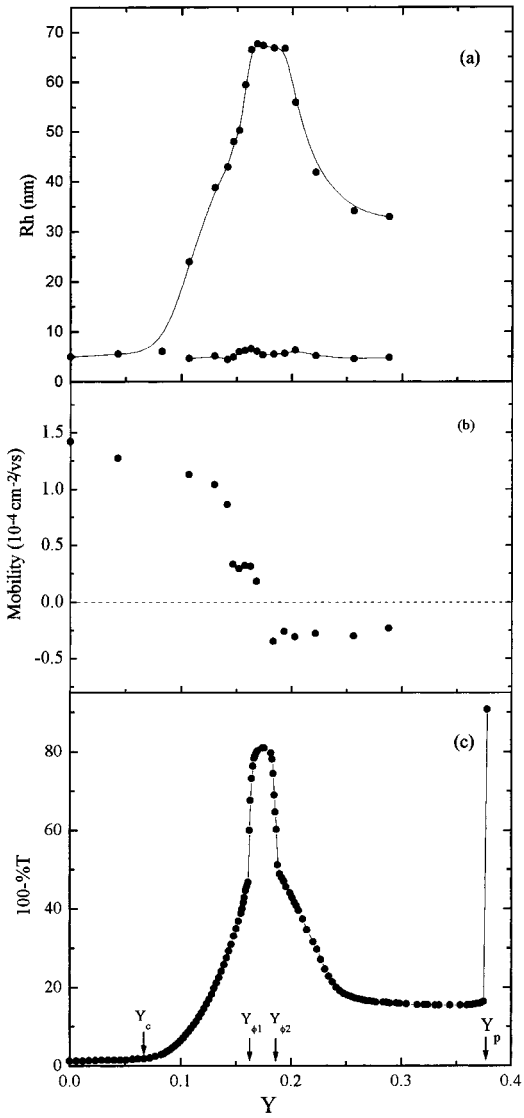

Figure 5. (a) Radius, (b) mobility, and (c) turbidity of PDADMAC/TX100−SDS in 0.10 M NaCl as a function of Y.

almost constant and the mobility only decreases with Y slightly, indicating that no interaction take place between polymer and micelles. Because the polymer concentration is very low relative to TX100, the small value of R_h arises mainly from the scattering of mixed micelles. Since micelles are nearly uncharged at low Y, the large positive mobility is mainly due to PDADMAC. The slight decrease in mobility is from the contribution of mixed TX100−SDS micelles which contain a very small fraction of SDS in this region. With further addition of SDS, an increase in size and a decrease in absolute mobility in region II ($Y_c < Y < Y_{\phi 1}$) provide strong evidence of complex formation. QELS yields a bimodal size distribution: in Figure 5a, the lower curve is the contribution from uncomplexed micelles, which remains essentially unchanged, while the upper curve shows that R_h of the complex changes with Y. During the coacervation range III ($Y_{\phi 1} < Y < Y_{\phi 2}$), the size of the complex becomes very large, and the mobility approaches zero. At $Y_{\phi 2} < Y < Y_p$ (region IV), we observe a significant decrease in size while the mobility becomes negative. When $Y \geq Y_p$ (region V), neither size or mobility can be measured because of limitations of the techniques in systems of large particles.

To explain this complex phase behavior and the accompanying effects of salt on coacervation, we first consider that the binding of anionic micelles to cationic polymers is a consequence of electrostatic attractive interactions. This binding leads to complex formation and reduction of the initially positive charge of the polyion. For different polyelectrolyte:micelle mixing ratios, the resulting complex can be intramolecular or intermolecular. For example, viscometric studies on SDS−cationic polymer systems by Goddard et al.[43,44] indicated that intermolecular association was promoted in solutions of high polymer concentration and intramolecular association was favored at low polymer concentration. Previous work of our group[17] on PDADMAC/TX100−SDS system suggested that intrapolymer complexes transform to interpolymer complexes with increasing polyelectrolyte concentration and that such high-order complex formation is the precursor of complex coacervation.

Although the above results and discussion provide some understanding of complex coacervation in polyelectrolyte/micelle systems, there has been no theoretical model developed specifically for this type of complex coacervation. However, several theoretical models have been presented for complex coacervation of polyelectrolyte mixtures. These models which may help us to obtain a plausible explanation for polyelectrolyte/micelle coacervation have been discussed and compared by Burgess.[23] The Voorn−Overbeek theory,[45−47] developed on the basis of the experimental data by of Bungenberg de Jong,[48] assumed a random chain distribution of macromoleculer in both phases, negligible solvent−solute interactions, and electrostatic interactive forces of a distributive nature. Here, "distributive" means that no site-specific interaction takes place in coacervation. According to this theory, the primary factors that affect coacervation are polyelectrolyte charge density and molecular weight. The formation of a concentrated coacervate phase is a spontaneous process and is driven by a gain in electrostatic free energy at the expense of a decrease in total entropy. The dilute phase aggregate model, developed by Veis and Aranyi,[49] proposed that complex coacervation occurred in two steps. First, oppositely charged polyelectrolytes aggregate by electrostatic interaction to form neutral aggregates of low configurational entropy, and then these aggregates rearrange to form coacervate. The ion-paired aggregates

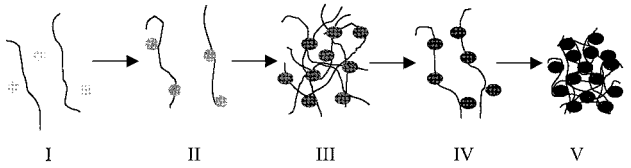

Figure 6. A simplified mechanism for five phases corresponding to phase diagram. The darker shade represents the higher charge density.

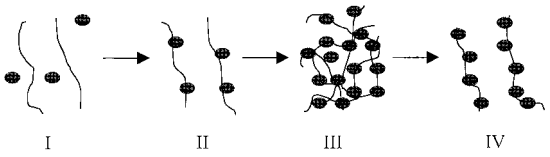

Figure 7. Simplified diagram for the phase changes with a decrease of salt concentration.

formed in the first step are present in both coacervate phase and equilibrium dilute phase. Coacervation is thought to be driven by the gain in configurational entropy when aggregates (corresponding to soluble complex in the present work) rearrange into a randomly distributed coacervation phase. The formation of soluble PDADMAC/TX100−SDS complexes under a wide range of conditions supports this model. A third model developed by Tainaka[50] also considered that aggregates, possibly neutral, are present in both phases, but without specific ion pairing. According to this model, coacervation is driven by attractive forces among aggregates. Both the charge density and the chain length of polyelectrolytes must fall within a certain range for coacervation to occur. If the charge density is too high or the chain length is too long, coprecipitation of the two polyelectrolytes will take place because of strong long-range attractive forces among aggregates. On the other hand, if the charge density is too low and the chain length is too short, the dilute solution is stabilized by short-range repulsive forces, and coacervation will not take place. These three models differ to some extent concerning the roles of electrostatic interaction, entropy, and the significance of solvent−solute interaction. None of these theories can describe all cases of complex coacervation. The Voorn−Overbeek theory and Veis and Aranyi theory are restricted to low charge density systems; the Tainaka theory, while applicable to both high and low charge density systems, does not provide a full explanation of coacervation process, such as suppression of coacervation at low ionic strength. However, these theories do provide a reasonable explanation for a large number of systems.

We now propose a simple mechanism consistent with the present phase behavior results for the PDADMAC/TX100−SDS system. Although the current system differs from those described by the previous theories, we also believe along with Veis and Aranyi that this coacervation involves attractive forces between neutral aggregates which in turn were formed by electrostatic interaction. The "cartoons" shown in Figure 6 correspond to the five phases in Figure 3, with circles representing mixed micelles and shading intensity corresponding to charge density. In region I, a single phase without complexes, the surface charge density of the TX100−SDS mixed micelles is not sufficient to lead to complex formation. Thus, turbidity, radius, and mobility all remain unchanged. With the addition of SDS, the charge density of the mixed micelles increases, which leads to soluble complex formation, as indicated by an increase in size and turbidity and a decrease in absolute mobility in region II. In this region, complexes carry positive charges. With further addition of SDS, more mixed micelles of progressively higher charge density bind, accompanied by a prominent increase in size and turbidity and a decrease in absolute mobility. Here, complex charges are electrically neutralized, which enables intrapolymer complexes to aggregate into interpolymer complexes, which in turn form coacervate. This is why the coacervation region III is centered at the charge neutralization point. With the addition of SDS beyond charge neutralization, the higher charge density of mixed micelles increases the intrinsic binding of micelles to polyelectrolytes. However, the higher charge density of mixed micelles also eventually produces electrostatic intermicellar repulsion and concomitant intercomplex repulsion. These two effects eventually lead in region IV to a redissolution of the interpolymer complexes into intrapolymer complexes with net negative charges. The electrostatic intermicellar repulsion could cause the number of mixed micelles bound per polymer chain $\bar{n}$ to decrease. The fact that the mobility in region IV is almost unchanged with addition of SDS might arise from the compensating effects of a decrease in $\bar{n}$ simultaneous with an increase in Y. Mixed micelles with very high charge density display a strong interaction with the polyelectrolytes in region V, leading to tight binding of micelles with polyelectrolytes. With the consequent loss of counterions and hydration, precipitation occurs. In summary, the charge density of mixed micelles may be the paramount controlling factor for coacervation in systems such as PDADMAC/TX100−SDS.

We now turn to the effect of salt on coacervation. As shown in Figures 3 and 4, the increase of salt concentration can move the system either from coacervate (region III) to either positively charged soluble complex (region II) or noninteracting phase (region I) or from negatively charged soluble complex (region IV) to coacervate. These "salt enhancement" and "salt suppression" effects can be plausibly explained by the model in Figure 7. The result from mobility measurements (Figure 5b) indicates that coacervation takes place at the charge neutralization point, which means that electrical neutrality is the most important requirement for coacervation. Thus, it is clear that coacervation requires the binding of some particular number of micelles to polyelectrolytes. Screening of electrostatic interactions between polyelectrolytes and micelles by salt means that the binding affinity of micelles to polyelectrolytes increases with a decrease in salt concentration. As the binding affinity increases, the system can change from one in which no micelles are bound (region I), to a positively charged complex with few bound micelles (region II), then to coacervate with the "right" number of micelles for net electroneutrality (region III), and finally to a negatively charged complex with excess bound micelles (region IV). Similarly, the addition of salt can move the system progressively from region IV to region I. Therefore, coacervation can be both "suppressed" and "enhanced" through changing the number of bound micelles. The decrease of binding affinity with increase of salt concentration also causes all phase boundaries Y_c, $Y_{\phi 1}$, $Y_{\phi 2}$, and Y_p to shift to larger Y.

From Figure 3, it is noted that the coacervation region shrinks with the decrease of salt concentration until at $I = 0.05$ M no coacervation is observed. This result can

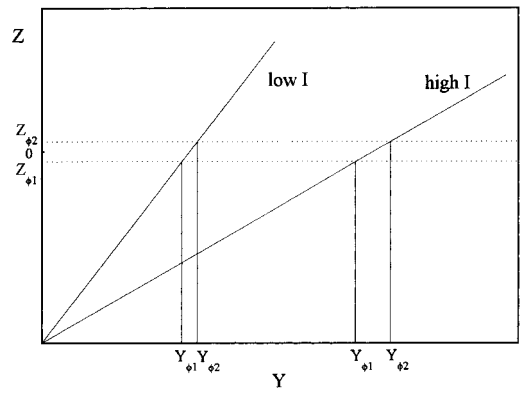

Figure 8. A schematic description of why cooacervation region with respect to *Y* shrinks with decrease of salt concentration *I*. When the net charge of complexes *Z* is located in the charge region between $Z_{\phi 1}$ and $Z_{\phi 2}$, coacervation takes place. The region between $Y_{\phi 1}$ and $Y_{\phi 2}$ is the coacervation region.

be explained in several ways, the first represented by the schematic diagram of Figure 8. According to the results in Figure 5, the coacervation region is centered at the charge neutralization point. Thus, when the net charge of the complexes *Z* is located in the range between $Z_{\phi 1}$ and $Z_{\phi 2}$, coacervation takes place. The lines indicated by "low *I*" and "high *I*" represent hypothetical relationships between the net complex charge and *Y* at low and high salt concentration, respectively. Because the binding affinity of micelles to polyelectrolytes increases with decrease in salt concentration, the change of the net complex charge with *Y* (dZ/dY) increases with the decrease of salt concentration. Because of stronger binding at lower salt concentration, the number of bound micelles is large so that coacervate is redissolved to negatively charged complexes even at very low *Y* value. Thus, from Figure 8, the coacervation region between $Y_{\phi 1}$ and $Y_{\phi 2}$ at low salt concentration is smaller than that at large salt concentration. At $I = 0.05$ M, the complex charge changes so quickly with *Y* that the coacervation has no chance to be observed.

A second possible explanation of the diminution of the coacervation region with the decrease of salt concentration is related to the size of TX100−SDS mixed micelles. The size of mixed micelles is strongly influenced by the SDS mole fraction *Y* and the ionic strength *I*.[51] The dependence of the size on *Y* and *I* is complicated; however, normally, micelles are larger at large (*Y*, *I*) than at low (*Y*, *I*). The hydrodynamic radii R_h of the mixed micelles at $Y = 0.40$ and $I = 0.60$ M, and at $Y = 0.17$ and $I = 0.10$ M, are 15.1 and 5.5 nm, respectively. Although the binding energy may be the same at different sets of *Y* and *I* along the I/II boundary, complexes formed at different positions may be structurally different. In particular, the lower curvature of micelles at smaller (*Y*, *I*) values could result in adsorption of polymer chains in flatter configurations than in the case for large, highly curved micelles. In the former case, more efficient ion-pairing could lead to lower hydration, allowing these complexes to coacervate more readily.

Conclusions

Turbidity, dynamic light scattering, and electrophoretic mobility were used to study the effects of salt concentration and charge density on coacervation of the PDADMAC/TX100−SDS polyelectrolyte/mixed micelle system. Liquid−liquid phase separation (coacervation) occurs when the electrophoretic mobility is close to zero. This corresponds to the binding of some specific number of micelles. Changes in salt concentration can decrease or increase the binding affinity of micelles to polyelectrolytes. Hence, coacervation can be both enhanced and suppressed by increasing or decreasing salt concentration. The present results also suggest the importance of the mixing charge ratio of micelles to polyelectrolytes. Further studies on the effects of polymer concentration, polymer molecular weight, and polymer:micelle stoichiometry are in progress.

Acknowledgment. This work was supported by NSF (DMR-9619722) and by Procter & Gamble Company. We thank Prof. Michael Fisher for helpful observations.

References and Notes

(1) Bungenberg de Jong, H. G. In *Colloid Science*; Kruyt, H. R., Ed.; Elsevier: Amsterdam, 1949; Vol. 2.
(2) Goddard, E. D. *J. Soc. Cosmet. Chem*. **1990**, *41*, 23.
(3) Kayes, J. B. *J. Pharm. Pharmacol*. **1977**, *29*, 163.
(4) Deasy, P. B. In *Microencapsulation and Related Drug Process*; Marcel Dekker: Basel, 1984.
(5) Oparin, A. I.; Gladilin, K. L.; Kirpotin, D. B.; Chertibrim, G. V.; Orlovsky, A. F. *Dokl. Acad. Nauk SSSR* **1997**, *232*, 485.
(6) Burgess, D. J. In *Macromolecular Complexes in Chemistry and Biology*; Dubin, P. L., Davis, R. M., Bock, J., Shulz, D., Thies, C., Eds.; Springer-Verlag: Berlin, 1994; p 285.
(7) Veis, A. In *Biological Polyelectrolytes*; Marcel Dekker: New York, 1970; Chaptor 4.
(8) Piculell, L.; Lindman, B. *Adv. Colloid Interface Sci*. **1992**, *41*, 149.
(9) Lindman, B.; Thalberg, K. In *Interaction of Surfactants with Polymers and Proteins*; Goddard, E. D., Ananthapadmanabhan, K. P., Eds.; CRC Press: Boca Raton, FL, 1993; Chapter 5.
(10) Li, Y.; Dubin, P. L. In *Structure and Flow in Surfactant Solutions*; Herb, C. A., Prud'homme, R. K., Eds.; ACS Symposium Series 578; American Chemical Society: Washington, DC, 1994; Chapter 23, p 320.
(11) Guillemet, F.; Piculell, L. *J. Phys. Chem*. **1995**, *99*, 9201.
(12) Ranganathan, S.; Kwak, J. C. T. *Langmuir* **1996**, *12*, 1381.
(13) Piculell, L.; Lindman, B.; Karlström, G. In *Polymer-Surfactant Systems*; Kwak, J. C. T., Ed.; Marcel Dekker: New York, 1998; p 65.
(14) Dubin, P. L.; Rigsbee, D. R.; McQuigg, D. W. *J. Colloid Interface Sci*. **1985**, *105*, 509.
(15) Dubin, P. L.; Oteri, R. *J. Colloid Interface Sci*. **1983**, *95*, 453.
(16) Li, Y.; Dubin, P. L.; Dautzenberg, H.; Lück, U.; Hartmann, J.; Tuzar, Z. *Macromolecules* **1995**, *28*, 6795.
(17) Li, Y.; Xia, J.; Dubin, P. L. *Macromolecules* **1994**, *27*, 7049.
(18) Xia, J.; Zhang, H. Rigsbee, D. R.; Dubin, P. L.; Shaikh, T. *Macromolecules* **1993**, *26*, 2759.
(19) Rigsbee, D. R.; Dubin, P. L. *Langmuir* **1996**, *12*, 1928.
(20) Sudbeck, E. A.; Dubin, P. L.; Curran, M. E.; Skelton, J. *J. Colloid Interface Sci.* **1991**, *142*, 512.
(21) Dubin, P. L.; Curran, M. E.; Hua, J. *Langmuir* **1990**, *6*, 707.
(22) McQuigg, D. W.; Kaplan, J. I.; Dubin, P. L. *J. Phys. Chem*. **1992**, *96*, 1973.
(23) Burgess, D. J. *J. Colloid Interface Sci*. **1990**, *140*, 227.
(24) Goddard, E. D.; Hannan, R. B. *J. Colloid Interface Sci*. **1976**, *55*, 73.
(25) Dubin, P. L.; Davis, D. D. *Macromolecules* **1984**, *17*, 1294.
(26) Dubin, P. L.; Davis, D. D. *Colloids Surf*. **1985**, *13*, 113.
(27) Dubin, P. L.; Rigsbee, D. R.; Gan, L.-M.; Fallon, M. A. *Macromolecules* **1988**, *21*, 2555.
(28) Dubin, P. L.; Thé, S. S.; McQuigg, D. W.; Chew, C. H.; Gan, L.-M. *Langmuir* **1989**, *5*, 89.
(29) Dubin, P. L.; Vea, M. E.; Fallon, M. A.; Thé, S. S.; Rigsbee, D. R.; Gan, L.-M. *Langmuir* **1990**, *6*, 1422.
(30) Dubin, P. L.; Thé, S. S.; McQuigg, D. W.; Gan, L.-M.; Chew, C. H. *Macromolecules* **1990**, *23*, 2500.
(31) Li, Y.; Dubin, P. L.; Havel, H. A.; Edwards, S. L.; Dautzenberg, H. *Langmuir* **1995**, *11*, 2486.
(32) Mizusaki, M.; Morishima, Y.; Dubin, P. L. *J. Phys. Chem. B* **1998**, *102*, 1908.
(33) Hayakawa, K.; Kwak, J. C. T. *J. Phys. Chem*. **1982**, *86*, 3866.

(34) Hayakawa, K.; Kwak, J. C. T. *J. Phys. Chem*. **1983**, *87*, 506.
(35) Malovikova, A.; Hayakawa, K.; Kwak, J. C. T. *J. Phys. Chem*. **1984**, *88*, 1930.
(36) Shirahama, K.; Tashiro, M. *Bull. Chem. Soc. Jpn*. **1984**, *57*, 377.
(37) Shirahama, K.; Masaki, T.; Takashima, K. In *Microdomains in Polymer Solutions*; Dubin, P. L., Ed.; Plenum: New York, 1985.
(38) Thalberg, K.; Lindman, B.; Karlström, G. *J. Phys. Chem*. **1991**, *95*, 6004.
(39) Hahn, M.; Jaeger, W. *Die Angew. Makromol. Chem*. **1992**, *198*, 165.
(40) Provencher, S. W. *Comput. Phys. Commun*. **1982**, *27*, 229.
(41) Miller, J. F.; Schätzel, K.; Vincent, B. *J. Colloid Interface Sci*. **1991**, *143*, 532.
(42) Tscharnuter, W. W.; McNeil-Watson, F.; Fairhurst, D. In *Particle Size Distribution III: Assessment and Characterization*; Provder, T., Ed.; ACS Symposium Series 693; American Chemical Society: Washington, DC, 1996; Chapter 23, p 327.
(43) Goddard, E. D.; Leung, P. S. *Polym. Prepr*. (*Am. Chem. Soc., Div. Polym. Chem*.) **1982**, *23*, 47.
(44) Goddard, E. D.; Hannan, R. B. In *Micellization, Solubilization and Microemulsions*, Mittal, K. L., Ed.; Plenum Press: New York, 1977; Vol. 2, p 835.
(45) Voorn, M. J. *Recl. Trav. Chim. Pays-Bas* **1956**, *75*, 317.
(46) Overbeek, J. Th. G.; Voorn, M. J. *J. Cell. Comput. Physiol*. **1957**, *49* (Suppl. 1), 7.
(47) Voorn, M. J. *Fortschr. Hochpolym.-Forsch*. **1959**, *1*, 192.
(48) Bungenberg de Jong, M. G. In *Colloid Science*; Kruyt, G. R., Ed.; Elsevier: New York, 1990; Vol. II, pp 335−432.
(49) Veis, A.; Aranyi, C. *J. Phys. Chem*. **1960**, *64*, 1203.
(50) Tainaka, K. *J. Phys. Soc. Jpn*. **1979**, *46*, 1899.
(51) Dubin, P. L.; Principi, J. M.; Smith, B. A.; Fallon, M. A. *J. Colloid Interface Sci*. **1989**, *127*, 558.

MA990972V